CHEMISTRY OF MATERIALS

Article

pubs.acs.org/cm

Triphenylamine Dendronized Iridium(III) Complexes: Robust Synthesis, Highly Efficient Nondoped Orange Electrophosphorescence and the Structure–Property Relationship

Minrong Zhu,[†] Jianhua Zou,[‡] Xun He,[†] Chuluo Yang,*[,†] Hongbin Wu,*[,‡] Cheng Zhong,[†] Jingui Qin,[†] and Yong Cao[‡]

[†]Department of Chemistry, Hubei Key Lab on Organic and Polymeric Optoelectronic Materials, Wuhan University, Wuhan 430072, People's Republic of China

[‡]Institute of Polymer Optoelectronic Materials and Devices, State Key Laboratory of Luminescent Materials and Devices, South China University of Technology, Guangzhou 510640, People's Republic of China

Supporting Information

ABSTRACT: New triphenylamine dendronized homoleptic Ir(III) complexes, namely **Ir-G1**, **Ir-G2**, and **Ir-G3**, with six, eighteen, and up to forty-two triphenylamine units, respectively, are designed and efficiently synthesized through convergent strategy. Both linear enlargement of the dendritic arms and the "double-dendron" strategy are applied to maximize the degree of site-isolation of the emissive center. The relationship between the dendritic structures and their photophysical, electrochemical, and electrophosphorescent performances is investigated. Phosphorescent organic light-emitting diodes (PhOLEDs) employing the dendrimers as solution-processed emitters are fabricated. The nondoped devices with **Ir-G1** and **Ir-G2** as emitters display very high efficiencies and small values of efficiency roll-off. For example, a device with **Ir-G1** as emitter exhibits the best results ever reported for solution-processed orange phosphorescent devices with maximum luminous efficiency of 40.9 cd A^{-1} and power efficiency of 39.5 lm W^{-1}. Moreover, the maximum power efficiency of the nondoped device is nearly three times higher than that of the doped control device by doping **Ir-G1** into the general polymer matrix. This indicates that incorporation of triphenylamine moieties into the sphere of iridium(III) core is a simple and effective approach to develop highly efficient host-free dendritic phosphors.

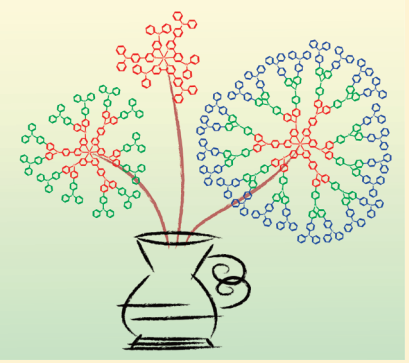

KEYWORDS: *iridium, dendrimer, synthesis, electrophosphorescence*

INTRODUCTION

Phosphorescent organic light-emitting diodes (PhOLEDs) unfurl a bright future for the next generation flat-panel displays and solid-state illumination sources due to their merit of high quantum efficiencies compared with fluorescent OLEDs.[1] The most efficient PhOLEDs have the guest emitter blended in a host matrix to prevent the luminescence quenching caused by aggregation of the emissive species.[2−4] However, the blending systems intrinsically suffer from the physical phase separation and hence deteriorate the device performance.[5]

Recently, the use of phosphorescent iridium-cored dendrimers appears to be an effective approach to fabricate host-free electrophosphorescent devices.[6] With numerable functional groups orderly attached to the periphery of the emissive center, the interactions between iridium cores can be controlled at the molecular level by the generation number and/or the dendron number of the dendrimer.[7] In particular, the "double-dendron" materials, which have two dentrons per ligand of the core, have enabled very efficient photoluminescence and electroluminescence from the neat films.[6e]

Considering the susceptibleness of the coordination between Ir(III) and organic ligand in many reaction conditions, most Ir(III) dendrimers have been prepared through a convergent strategy, which can give rise to a structure that is precisely defined, is of high purity, and is without ill-defined end groups.[8] However, the complexation of dendronized ligands with Ir(III) salts in a typical reaction medium of glycerol usually results in very discouraging yields in the range of 10−35% due to the stiff and hardly soluble branching units.[7a] To improve the solubility of the large dendronized ligands, surface groups such as alkyl or alkoxy chains have to be attached, which could impair the charge mobility and create difficulties during the reaction and purification of the intermediate stages. Coming to the second-, third-, and higher generations, the synthetic demands can grow significantly with decreasing yields and increasing probability of structural defects.[7b] Hence, preparation of high generation Ir(III) dendrimers bearing dense dendrons remains a synthetic challenge and major obstacle to application.

In this contribution, we present the robust synthesis of the triphenylamine dendronized homoleptic Ir(III) dendrimers

Received: September 13, 2011
Revised: November 27, 2011
Published: November 27, 2011

   dx.doi.org/10.1021/cm202732j | *Chem. Mater.* 2012, 24, 174–180

through traditional convergent strategy. The dendrimers are denoted as **Ir-G1**, **Ir-G2**, and **Ir-G3**, with six, eighteen, and up to forty-two triphenylamine units, respectively (Figure 1).

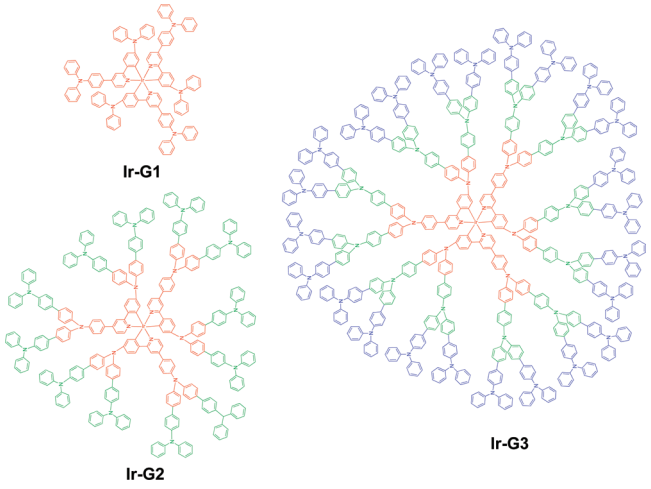

Figure 1. Ir(III)-cored dendrimers of first-generation (**Ir-G1**), second-generation (**Ir-G2**), and third-generation (**Ir-G3**).

Triphenylamine units possess a high HOMO level (ca. −5.2 eV) and sufficiently high triplet energy (ca. 2.9 eV), and hence they can be used as good antenna for the charge transfer and/or energy transfer to the emitting center.[9] What is more, without any solubilizing side groups, the dendritic triphenylamine compounds have good solubility in common organic solvents.[10] All these merits make triphenylamine groups highly appealing as desirable branching units for construction of dendritic Ir(III) phosphors. Unprecedentedly, we achieved very efficient complexation between the iridium and the bulky dendritic ligands by the optimization of reaction medium. To the best of our knowledge, the third generation dendrimer (**Ir-G3**) is the first report covering the highest loading functional dendrons among the iridium phosphors.[7d] The relationship between the dentritic structures and their photophysical, electrochemical, and electrophosphorescent performances is discussed. The nondoped device with **Ir-G1** as emitter exhibits the best results ever reported for solution-processed orange phosphorescent devices. Moreover, the maximum power efficiency of the nondoped device is nearly three times higher than that of the doped control device.

EXPERIMENTAL SECTION

General Information. ^{1}H NMR and ^{13}C NMR spectra were measured on a MECUYR-VX300 spectrometer. Elemental analyses of carbon, hydrogen, and nitrogen were performed on a Vario EL III microanalyzer. MALDI-TOF mass spectra were performed on Bruker BIFLEX III TOF mass spectrometer. Gel permeation chromatography (GPC) measurements were recorded relative to a polystyrene standard using a Waters 515 HPLC equipped with MZ gel SDplus linear 500 Å column at 30 °C. THF was used as eluent at a flow rate of 1.0 mL min^{-1}. UV−vis absorption spectra were conducted on a Shimadzu UV-2500 recording spectrophotometer. Photoluminescent spectra were recorded on a Hitachi F-4500 fluorescence spectrophotometer. The lifetimes of phosphorescence in toluene solution were measured by exciting the materials with 350 nm from a Hydrogen lamp on a FLS 920 Combined steady-state and lifetime spectrometer. Differential scanning calorimetry (DSC) was performed on a NETZSCH DSC 200 PC unit at a heating rate of 10 °C min^{-1} from room temperature to 400 °C under a flow of nitrogen. The glass transition temperature was determined from the second heating scan. The glass transition temperature of **Ir-G1** appears at 217.2 °C, and no obvious thermal transition was observed for **Ir-G2** and **Ir-G3**. Cyclic voltammetry (CV) was carried out in nitrogen-purged dichloromethane (oxidation scan) at room temperature with a CHI voltammetric analyzer. Tetrabutylammonium hexafluorophosphate (TBAPF6) (0.1 M) was used as the supporting electrolyte. The conventional three-electrode configuration consists of a platinum working electrode, a platinum wire auxiliary electrode, and an Ag wire pseudoreference electrode with ferrocenium−ferrocene (Fc^{+}/Fc) as the internal standard. Cyclic voltammograms were obtained at a scan rate of 100 mV s^{-1}. The onset potential was determined from the intersection of two tangents drawn at the rising and background current of the cyclic voltammogram. The calculation for **Ir-G1** was performed at the density functional theory (DFT) level with the B3LYP functional. A double-quality basis set consisting of Hay and Wadt's effective core potentials (LANL2DZ) was employed for Ir atom and a 6-31G(d) basis for other elements. The **Ir-G2** was constructed based on **Ir-G1** and then optimized with Merck Molecular Force Field with the metal core frozen due to the lack of force field parameter for Ir(III). The structure of **Ir-G3** was built on the optimized **Ir-G2** structure with a molecular mechanics method using Merck Molecular Force Field under the same procedure. Then the closest contacts between dendrons were measured with the threshold of 4.6 Å.

Device Fabrication and Measurement. Patterned indium tin oxide (ITO)-coated glass substrates with a sheet resistance of 15−20 ohm/square underwent a wet-cleaning course in an ultrasonic bath, beginning with acetone, followed by detergent, deionized water, and isopropanol. After oxygen-plasma treatment, a 50 nm thick anode buffer layer of PEDOT:PSS (Baytron P4083, Bayer AG) film was spin-cast on the ITO substrate and dried by baking in vacuum oven at 80 °C overnight. The emitting layer was prepared by spin-coating from chlorobenzene solution on top of the PEDOT layer and then annealed at 100 °C for 20 min. TPBI (25 nm), Ba (4 nm), and Al (150 nm) were evaporated with a shadow mask successively at a base pressure of 3×10^{-4} Pa. The thickness of the evaporated TPBI and cathode was monitored by a quartz-crystal thickness/ratio monitor (Sycon model STM-100/MF). The cross-sectional area between the cathode and anode defined the pixel size of 19 mm^2. Except for the spin coating of the PEDOT layer, all the processes were carried out in the controlled atmosphere of a nitrogen drybox (Vacuum Atmosphere Co.) containing less than 1 ppm oxygen and moisture. All measurements were carried out at room temperature under ambient conditions.

Materials and Synthesis. Starting chemicals and reagents were purchased from commercial sources and used as received without further purification. Solvents for synthesis were purified according to standard procedures prior to use. All reactions were performed under an inner argon atmosphere. Synthesis of 4-(diphenylamino)-phenylboronic acid (**1**) was performed following the literature procedure.[12]

Synthesis of LG1. To a well degassed solution of 2,4-dibromopyridine (1.69 g, 7.15 mmol), **1** (5.40 g, 18.60 mmol), and 2 M Na_2CO_3 (45 mL, 22.50 mmol) in a mixed solvent of toluene (135 mL) and ethanol (45 mL) was added $Pd(PPh_3)_4$ (0.50 g, 0.43 mmol). The resulting mixture was stirred and heated to reflux at 110 °C for 48 h under argon atmosphere. After cooling to room temperature, the solvent was evaporated under reduced pressure and taken up with CH_2Cl_2. The organic layer was washed with brine and water sequentially and dried over anhydrous Na_2SO_4. After having been filtered, the solvent was evaporated to dryness and subjected to column chromatography on silica gel with petroleum/ethyl acetate (5:1, v/v) as the eluent to give the product (3.53 g) in a yield of 87% as an off white solid. ^{1}H NMR (300 MHz, $CDCl_3$): δ 8.65 (d, J = 5.1 Hz, 1H), 7.91 (d, J = 8.1 Hz, 2H), 7.83 (s, 1H), 7.57 (d, J = 8.1 Hz, 2H), 7.36 (d, J = 5.1 Hz, 1H), 7.29−7.24 (m, 8H), 7.16 (d, J = 7.5 Hz, 12H), 7.09 (d, J = 7.8 Hz, 2H), 7.04 (d, J = 7.2 Hz, 2H); ^{13}C NMR (75 MHz, $CDCl_3$): δ 162.80, 155.14, 154.25, 152.88, 152.65, 136.83, 134.81, 134.61, 133.22, 133.17, 130.35, 130.19, 128.92, 128.66, 128.33, 124.32, 122.72; MALDI-TOF: Calcd. for $C_{41}H_{31}N_3$ 565.70; Found

dx.doi.org/10.1021/cm202732j | *Chem. Mater.* 2012, 24, 174−180

Scheme 1. Synthesis of the Dendritic Ligands[a]

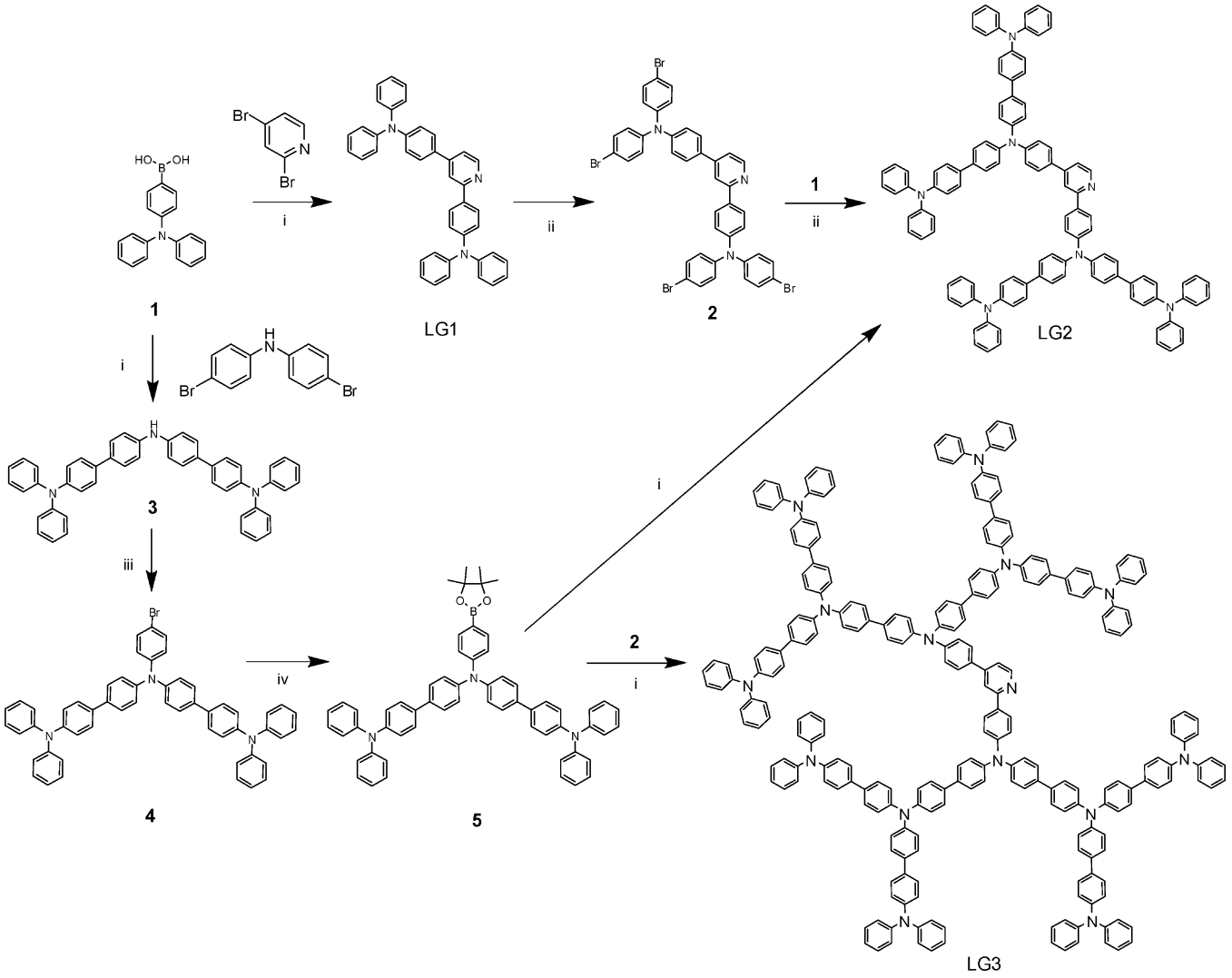

[a]Reagents and conditions: i) [$Pd(PPh_3)_4$], toluene, ethanol, 2 M base, reflux; ii) NBS, DMF, 0 °C, 80%; iii) 1-bromo-4-iodobenzene, CuI, (±)-*trans*-1,2-diaminocyclohexane, KO*t*Bu, 1,4-dioxane, 110 °C, 90%; iv) [$Pd(dppf)Cl_2$] (dppf = 1,1′-bis(diphenylphosphanyl)ferrocene), bis(pinacolato)-diboron, KOAc, 1,4-dioxane, 85 °C, 88%.

565.05; Anal. Calcd. for $C_{41}H_{31}N_3$: C 87.05, H 5.52, N 7.43; Found: C 86.84, H 5.58, 7.33.

Synthesis of 2. A solution of NBS (2.62 g, 14.74 mmol) in DMF (30 mL) was slowly added to a mixture of **LG1** (1.99 g, 3.51 mmol) in DMF (30 mL) with several drops of acetic acid at 0 °C under argon atmosphere. The resulting mixture was allowed to slowly warm up to room temperature to stir for another 18 h. To the solution was added H_2O (300 mL), and then the solution extracted with CH_2Cl_2 (300 mL). The organic layer was washed with $NaHCO_3$ saturated solution and dried over anhydrous Na_2SO_4. After removal of the solvent, the resulting solid was recrystallized from CH_2Cl_2 and ethanol twice to give a light yellow powder (2.47 g) in a yield of 80%. ^{1}H NMR (300 MHz, $CDCl_3$): δ 8.67 (d, J = 5.1 Hz, 1H), 7.94 (d, J = 8.7 Hz, 2H), 7.82 (s, 1H), 7.59 (d, J = 8.4 Hz, 2H), 7.40−7.35 (m, 9H), 7.15 (d, J = 8.7 Hz, 4H), 7.00−6.97 (m, 8H); ^{13}C NMR (75 MHz, $CDCl_3$): δ 162.07, 154.71, 153.52, 152.94, 151.06, 150.85, 138.95, 137.51, 137.43, 133.08, 131.00, 130.81, 128.64, 124.27, 122.58, 121.35, 121.01; MALDI-TOF: Calcd. for $C_{41}H_{27}Br_4N_3$ 881.29; Found 881.65.

Synthesis of 3. To a well degassed solution of 4-(diphenylamino)phenylboronic acid (5.46 g, 18.80 mmol) and bis(4-bromophenyl)amine (2.46 g, 7.50 mmol) and 2 M Na_2CO_3 (30 mL, 15.0 mmol) in toluene (90 mL) was added $Pd(PPh_3)_4$ (0.26 g, 0.23 mmol). The resulting mixture was stirred and heated to reflux at 110 °C for 48 h under argon atmosphere. After having been cooled to room temperature, the solvent was evaporated under reduced pressure and taken up with CH_2Cl_2. The organic layer was washed with brine and water sequentially and dried over anhydrous Na_2SO_4. After having been filtered, the solvent was evaporated to dryness and subjected to column chromatography on silica gel with petroleum/chloroform (2:1, v/v) as the eluent to give the product (4.18 g) in a yield of 85% as a white solid. ^{1}H NMR (300 MHz, $CDCl_3$): δ 7.40−7.16 (m, 10H), 7.13−6.84 (m, 26H); ^{13}C NMR (75 MHz, $CDCl_3$): δ 153.04, 152.34, 138.29, 135.18, 133.01, 131.56, 129.05, 128.62, 127.15; MALDI-TOF: Calcd. for $C_{48}H_{37}N_3$ 655.83; Found 655.23.

Synthesis of 4. Potassium *tert*-butoxide (0.97 g, 8.60 mmol) was added to a 100 mL round-necked flask containing **3** (3.78 g, 5.76 mmol), 1-bromo-4-iodobenzene (1.96 g, 6.92 mmol), and CuI (0.12 g, 0.58 mmol) under a flow of argon, and then (±)-*trans*-1,2-diaminocyclohexane (137 μL, 1.14 mmol) and 1,4-dioxane (40 mL) were added with syringe in sequence. The mixture was heated to 110 °C with good stirring overnight under argon atmosphere. After cooling, H_2O (100 mL) was added, and the mixture was extracted with CH_2Cl_2. The organic layer was combined and washed with H_2O and then dried over anhydrous Na_2SO_4. After the solvent was evaporated, the residue was purified by column chromatography on silica gel with petroleum/chloroform (2:1, v/v) to give a gray solid (4.20 g) with a

dx.doi.org/10.1021/cm202732j | *Chem. Mater.* 2012, 24, 174−180

yield of 90%. ^{1}H NMR (300 MHz, $CDCl_3$): δ 7.45 (d, J = 7.8 Hz, 8H), 7.26−7.21 (m, 14H), 7.11−7.00 (m, 12H), 6.99−6.86 (m, 6H); ^{13}C NMR (75 MHz, $CDCl_3$): δ 152.46, 151.71, 150.60, 139.26, 137.04, 134.07, 132.16, 129.19, 128.81, 127.70; MALDI-TOF: Calcd. for $C_{54}H_{40}BrN_3$ 810.82; Found 811.10.

Synthesis of 5. **4** (3.09 g, 3.82 mmol), bis(pinacolato)diborane (1.27 g, 5.0 mmol), and KOAc (1.37 g, 14.0 mmol) were mixed together in a 100 mL flask. After degassing, dioxane (40 mL) was added to the mixture under flow of argon. Afterward, $[Pd(dppf)Cl_2]$ (50 mg) was added. The reaction mixture was kept at 85 °C overnight under argon atmosphere and then cooled to room temperature. The solvent was concentrated, and the inorganic salt was dissolved completely after addition of water. After having been extracted with CH_2Cl_2, the combined organic layer was washed with brine and dried over anhydrous Na_2SO_4. The solvent was evaporated under reduced pressure, and the residue was purified through column chromatography with petroleum/CH_2Cl_2 (1:1, v/v) as the eluent to give the desired compound as a white solid (2.82 g) with a yield of 88%. ^{1}H NMR (300 MHz, $CDCl_3$): δ 7.68 (d, J = 7.5 Hz, 2H), 7.46 (d, J = 8.0 Hz, 8H), 7.26−7.25 (m, 12H), 7.18−7.11 (m, 14H), 7.04 (t, J = 7.5 Hz, 4H), 1.33 (s, 12H); ^{13}C NMR (75 MHz, $CDCl_3$): δ 151.77, 150.94, 150.18, 140.02, 139.63, 138.65, 133.34, 131.64, 129.11, 128.42, 128.12, 126.94, 126.24, 87.68, 28.97; MALDI-TOF: Calcd. for $C_{60}H_{52}BN_3O_2$ 857.88; Found 857.30.

Synthesis of LG2. According to the similar procedure for the preparation of **LG1**, **LG2** was synthesized by the Suzuki coupling of **5** with 2,4-dibromopyridine (or the 4-fold Suzuki coupling of tetrabromide **2** with 1 using Cs_2CO_3 as base) to give a yield of 80% (86%). ^{1}H NMR (300 MHz, $CDCl_3$): δ 8.67 (d, J = 5.4 Hz, 1H), 7.97 (d, J = 9.0 Hz, 2H), 7.87 (s, 1H), 7.62 (d, J = 8.4 Hz, 2H), 7.52−7.45 (m, 16H), 7.39 (d, J = 5.1 Hz, 1H), 7.28−7.20 (m, 32H), 7.14 (d, J = 9.0 Hz, 20H), 7.04 (t, J = 7.5 Hz, 8H); ^{13}C NMR (75 MHz, $CDCl_3$): δ 153.84, 152.61, 151.90, 150.81, 140.92, 139.57, 134.23, 132.96, 132.35, 130.14, 129.94, 129.38, 129.01, 128.13, 127.95; MALDI-TOF: Calcd. for $C_{113}H_{83}N_7$ 1538.92; Found 1538.33; Anal. Cacld. for $C_{113}H_{83}N_7$: C 88.19, H 5.44, N 6.37; Found: C 87.70, H 5.50, N 6.33.

Synthesis of LG3. The compound was prepared by the 4-fold Suzuki coupling of **5** with **2** similar to the procefure for **LG2** with a yield of 50%. ^{1}H NMR (300 MHz, $CDCl_3$): δ 8.64 (s, 1H), 7.97 (s, 2H), 7.88 (s, 1H), 7.60−7.44 (m, 51H), 7.40−7.23 (m, 62H), 7.21−7.11 (m, 40H), 7.05−7.00 (m, 30H); ^{13}C NMR (300 MHz, $CDCl_3$): δ 147.97, 147.07, 146.65, 135.34, 134.86, 129.57, 127.62, 124.61, 124.37, 123.14; MALDI-TOF: Calcd. for $C_{257}H_{187}N_{15}$ 3485.34; Found 3486.09; Anal. Calcd. for $C_{257}H_{187}N_{15}$: C 88.56, H 5.41, N 6.03; Found: C 88.29, H 5.52, N 5.86.

Preparation of Ir-G1. **LG1** (0.96 g, 1.70 mmol) and $Ir(acac)_3$ (0.25 g, 0.50 mmol) were precisely weighted up and added to a 50 mL round-necked flask. Thereafter, distilled *o*-dichlorobenzene (5 mL) was first added to the mixture. After the ligand was completely dissolved, 2-(2-methoxyethoxy)ethanol (10 mL) and glycerol (20 mL) were added to the flask. The mixture was refluxed at 230 °C for 24 h. After completion, *o*-dichlorobenzene was removed under reduced pressure. The mixture was poured into H_2O and extracted with CH_2Cl_2. The organic phase was washed with brine and dried over anhydrous Na_2SO_4. The solvent was evaporated under reduced pressure, and the residue was purified through column chromatography with petroleum/CH_2Cl_2 (1:1, v/v) as eluent to afford **Ir-G1** (0.95 g) as a red powder with a yield of 95%. ^{1}H NMR (300 MHz, $CDCl_3$): δ 7.85 (s, 3H), 7.61 (s, 3H), 7.52 (d, J = 8.0 Hz, 6H), 7.38 (d, J = 9.0 Hz, 3H), 7.29 (d, J = 9.0 Hz, 14H), 7.16−7.09 (m, 28H), 6.98 (s, 6H), 6.85−6.80 (m, 16H), 6.64 (s, 5H), 6.25 (d, J = 7.8 Hz, 6H); ^{13}C NMR (75 MHz, $CDCl_3$): δ 166.57, 149.19, 148.44, 147.91, 147.49, 147.28, 138.06, 131.42, 130.61, 129.67, 128.81, 127.85, 125.77, 125.01, 124.62, 123.85, 123.06, 122.37, 118.51, 114.85; MALDI-TOF: Calcd. for $C_{123}H_{90}IrN_9$ 1886.31; Found 1886.01; Anal. Calcd. for $C_{123}H_{90}IrN_9$: C 78.32, H 4.81, N 6.68; Found: C 78.28, H 4.88, N 5.86. M_w/M_n = 1.02.

Preparation of Ir-G2. **Ir-G2** was prepared following the procedure described for **Ir-G1**. The product was obtained as an orange-red powder (0.84 g) with a yield of 98%. ^{1}H NMR (300 MHz, $CDCl_3$): δ 7.89 (s, 3H), 7.67 (s, 3H), 7.59 (d, J = 9.0 Hz, 6H), 7.51−7.43 (m, 28H), 7.25 (d, J = 6.9 Hz, 80H), 7.20−7.11 (m, 46H), 7.04−6.91 (m, 58H), 6.81 (d, J = 8.7 Hz, 16H), 6.25−6.20 (m, 6H); ^{13}C NMR (75 MHz, $CDCl_3$): δ 147.97, 147.18, 146.57, 146.13, 136.08, 135.23, 134.66, 129.52, 127.79, 127.63, 127.42, 126.96, 125.33, 124.61,124.39, 124.22, 123.15, 122.83; MALDI-TOF: Calcd. for $C_{339}H_{246}IrN_{21}$ 4805.94; Found 4805.80; Anal. Calcd. for $C_{339}H_{246}IrN_{21}$: C 84.72, H 5.16, N 6.12; Found: C 84.47, H 5.31, N 6.11. M_w/M_n = 1.01.

Preparation of Ir-G3. **Ir-G3** was prepared following the procedure described for **Ir-G1**. The product was obtained as a yellow solid (0.25 g) with a yield of 50%. ^{1}H NMR (300 MHz, $CDCl_3$): δ 7.80−7.50 (m, 15H), 7.46−7.35 (m, 126H), 7.18−7.14 (m, 123H), 7.02−6.91 (m, 288H), 6.34−6.12 (m, 6H); ^{13}C NMR (75 MHz, $CDCl_3$): δ 137.23, 133.16, 129.77, 127.22, 125.15, 122.67; MALDI-TOF: Calcd. for $C_{771}H_{558}IrN_{45}$ 10645.20; Found 10649.04; Anal. Calcd. for $C_{771}H_{558}IrN_{45}$: C 86.99, H 5.28, N 5.92; Found: C 87.03, H 5.12, N 5.55. M_w/M_n = 1.05.

RESULTS AND DISCUSSION

Preparation and Characterization. The synthetic route for the dendritic chelating ligands is outlined in Scheme 1. The first-generation triphenylamine-based ligand (**LG1**) was facilely prepared through the Suzuki-coupling reaction of 4-(diphenylamino)phenylboronic acid (**1**) with commercially available 2,4-dibromopyridine.[12a] Initially, the stepwise preparation of second-generation counterpart (**LG2**) commenced with the synthesis of **3**, which was then subjected to a modified, mild Buchwald cross-coupling methodology to generate **4** in 90% yield.[12b] In this step, the selective amination of the aryl iodide in 1-bromo-4-iodobenzene was performed by using a powerful catalyst system comprised of CuI and racemic *trans*-1,2-cyclohexanediamine in the presence of KO*t*Bu. Subsequent borylation using bis(pinacolato)diboron afforded the desired pinacol boronic ester **5** in 88% yield. The Suzuki−Miyaura cross-coupling of building block **5** with 2,4-dibromopyridine gave the LG2 in 80% yield. Alternatively, direct 4-fold Suzuki coupling of **1** with aryl tetrabromide **2**, which was converted by treating LG1 with NBS (4 equivalent), also furnished the ligand bearing six triphenylamine units successfully. Following the same strategy, the third-generation analogue (**LG3**) was obtained in a yield of 50% by the Suzuki coupling of **5** with **2**. This efficient approach rendered it suitable for building up high generation dendrons without structural defect. The final step in the preparation of **Ir-G(1-3)** is the complexation of large all-aromatic ligands with an iridium source.[13] For the convenience and retrenchment of ligands, the standard one-pot procedure favors the preparation of homoleptic Ir(III) complexes, which involves treating $Ir(acac)_3$ (acac = 2,4-pentanedionate) with 3.2 equiv of free ligand in glycerol at refluxing temperature. Considering the moderate solubility of polytriphenylamine ligands in glycerol and high temperature required for the formation of desired facial configuration, *o*-dichlorobenzene and 2-(2-methoxyethoxy)ethanol were added as cosolvents proportionally. Consequently, the complexations for **Ir-G1** and **Ir-G2** were accomplished in nearly quantitative yields. Moreover, 50% of yield was obtained for **Ir-G3** bearing 42 triphenylamine branching units without difficulty from steric crowding. We assume that this robust coordination could be contributed from the decreased viscosity in the mixed solvent systems as well as the inherent good solubility of the triphenylamine-based ligands. This judicious choice of dendron source and reaction medium renders the gram-scale preparation

dx.doi.org/10.1021/cm202732j | *Chem. Mater.* 2012, 24, 174−180

of sophisticated iridium dendrimers feasible and contributes to their potential applications in plastic electronics.

The good solubility of the dendrimers in common solvents facilitates their purification and structural characterization. The molecular ion peaks in MALDI-TOF mass spectra verified the presence of the desired dendrimers. Furthermore, gel permeation chromatography (GPC) data exhibited a stepwise decrease of elution time as the generation grew (Figure 2). A

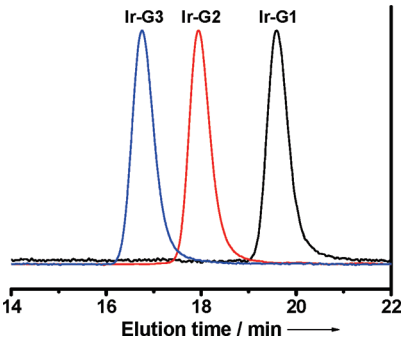

Figure 2. GPC traces for Ir-cored dendrimers in THF.

narrow polydispersity index (PDI) (1.01−1.05) indicates their purity. Also, the dendrimers were fully characterized by ^{1}H, ^{13}C NMR spectroscopy and elemental analysis.

Photophysical Properties. The absorption spectra of the dendrimers in toluene and the photoluminescence (PL) spectra of the dendrimers in toluene and films are presented in Figure

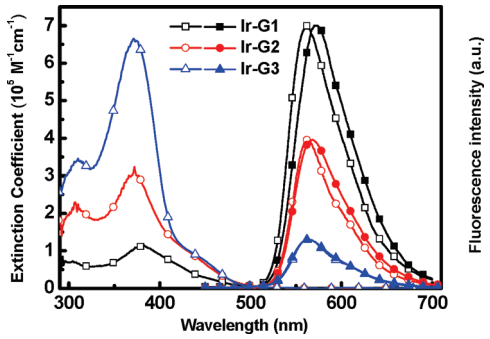

Figure 3. Electronic absorption spectra of dendrimers in toluene and their emission spectra recorded both in toluene (open) and film state (solid). The emission scale is arbitrary, and the spectra have been normalized and offset for comparison.

3. The photophysical data are summarized in Table 1. The absorptions around 300 and 380 nm for the dendrimers can be assigned to triphenylamine-centered $\pi-\pi^*$ and spin-allowed intraligand $\pi-\pi^*$ transitions, respectively, which are significantly enhanced in intensity with the increasing number of triphenylamine units. The weak features in the range of 380−500 nm come from the metal-to-ligand charge transfer (MLCT) states of the complexes.[7b]

The three dendrimers exhibit almost the same emission peak at ca. 561 nm in toluene solution, but **Ir-G3** displays a reduced emission red-shift of 2 nm from solution to film compared to 10 nm of **Ir-G1** and 6 nm of **Ir-G2**, which is indicative of a significantly reduced interaction between emissive cores with the increasing generation number.[14] Furthermore, the solution PL quantum yields (PLQYs) were measured in N_2-saturated toluene solutions by a relative method using *fac*-Ir(ppy)$_3$ (Φ_{FL} = 40%, in toluene) as reference,[15] and the relative PLQYs of dendrimers increase from 29% for **Ir-G1**, 40% for **Ir-G2**, to 44% for **Ir-G3**, respectively, indicating improving chromophore separation with the increasing generation number.

Electrochemical Characterization. The electrochemical property of the dendrimers was probed by cyclic voltammetry (CV), using tetrabutylammonium hexafluorophosphate ($TBAPF_6$) as the supporting electrolyte and ferrocene as the internal standard. The highest occupied molecular orbital (HOMO) energy levels of the dendrimers were determined from the onset of the oxidation potentials with regard to the energy level of ferrocene (4.8 eV below vacuum), and the lowest occupied molecular orbital (LUMO) levels were deduced from the HOMO energy levels and energy gaps determined by the onset of absorption. The HOMO and LUMO levels for **Ir-G1** were estimated to be −4.72 and −2.39 eV, respectively, and the HOMO levels of **Ir-G2** and **Ir-G3** were estimated to be higher than −5.0 eV but lower than that of Ir-G1. It would be ambiguous to obtain exact values of HOMO and LUMO levels for **Ir-G2** and **Ir-G3** since the first oxidation potential around 0.10 eV that corresponds to the oxidation of iridium core became too weak to be recognized (Figure S1, see the Supporting Information).[6d] Extra oxidation waves at higher potentials can be ascribed to the oxidation of the periphery dendrons, indicating that the polytriphenylamine-based dendrons could directly participate in the charge transport process.[7a]

Nondoped Orange Electrophosphorescence. To evaluate the performance of the three dendrimers as self-host phosphorescent emitters, nondoped PhOLEDs were fabricated with the following configurations: ITO/poly-

Table 1. Photophysical Properties and Electroluminescent Characteristics of Phosphorescent Dendrimers

dendrimer	λ_{max} [a] [nm] (ε*10^{-5})	λ_{em} [b] [nm]	λ_{em} [c] [nm]	τ [d] (ns)	$V_{turn-on}$ [e] [V]	$\eta_{c.\ max}$ [f] [cd/A)]	$\eta_{p.\ max}$ [g] [lm/W]	$\eta_{ext.\ max}$ [h] [%]	CIE[I] x, y
Ir-G1	304 (0.7),	561	571	10.5	2.8	40.9	39.5	16.4	0.50, 0.48
	376 (1.2).					35.7	31.6	14.6	
Ir-G2	308 (2.3),	562	568	10.3	3.0	38.9	38.3	15.6	0.52, 0.47
	370 (3.2).					32.1	28.8	12.9	
Ir-G3	310 (3.5),	562	564	16.7, 36.4	3.9	7.6	5.4	3.0	0.48, 0.50
	371 (6.7).					4.8	1.2	1.8	

[a]Measured in toluene solution with concentrations of 3.39, 1.27, and 0.43 *10^{-5} M for **Ir-G1**, **Ir-G2**, and **Ir-G3**, respectively. Extinction coefficients are given in parentheses. [b]Measured in toluene at 298 K with a concentration of 10^{-5} M and the excitation wavelength of 380 nm. [c]Neat film data measured at 298 K with the excitation wavelength of 380 nm. [d]Measured in toluene at a concentration of 10^{-5} M at 298 K. [e]At a brightness of 1 cd m^{-2}. [f]Maximum current efficiency, then data at 1000 cd m^{-2}. [g]Maximum power efficiency, then data at 1000 cd m^{-2}. [h]Maximum external quantum efficiency, then data at 1000 cd m^{-2}. [I]CIE at 7 V.

dx.doi.org/10.1021/cm202732j | *Chem. Mater.* 2012, 24, 174−180

(ethylenedioxythiophene):poly(styrene sulfonic acid) (PEDOT:PSS, 50 nm)/**Ir-G1**, **Ir-G2**, or **Ir-G3** (80 nm)/1,3,5-tris(2-*N*-phenylbenzimidazolyl)benzene (TPBI, 25 nm)/Ba (4 nm)/Al (150 nm) (Figure S2, see the Supporting Information). In this sandwich geometry, TPBI acts as an electron-transporting and hole-blocking material. The electroluminescence (EL) devices display the consistent spectra with their PL counterparts, without additional emission from the aggregation or the dendrons. The current−voltage−luminance (J−V−L) characteristics and efficiency versus current density curves are depicted in Figure 4, and the main device data are collected in

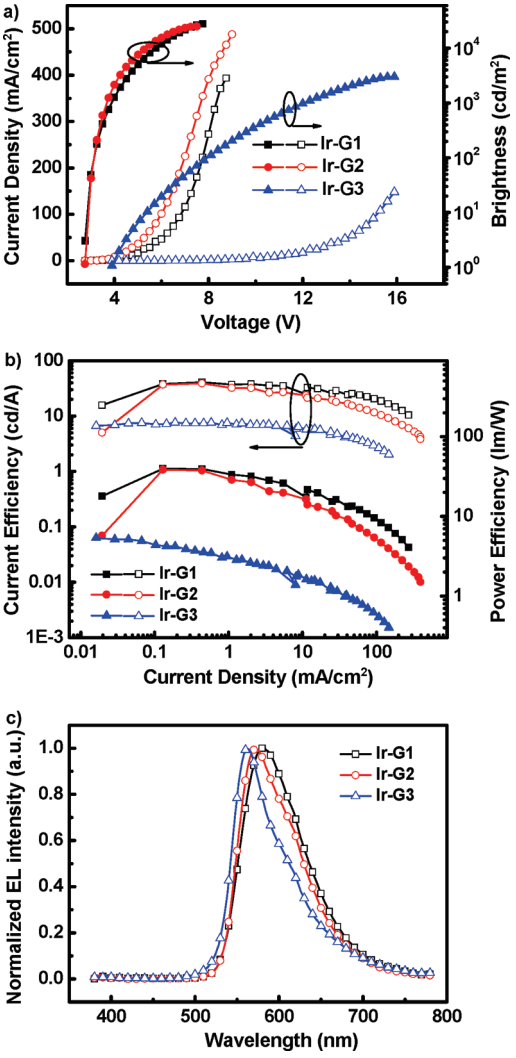

Figure 4. The J−V−L characteristics (a), current/power efficiency versus current density curves (b), and EL spectra of dendrimers at a driving voltage of 7 V (c).

Table 1. The low turn-on voltages in a range of 2.8−3.9 eV are realized due to the reduced energy barrier between anode and emission layer, as evidenced by the fact that HOMO levels of the three dendrimers are close to the work function of the hole-injection layer of PEDOT (−4.80 eV). The device from **Ir-G1** achieves a maximum current efficiency ($\eta_{c.\,max}$) of 40.9 cd A^{-1}, a maximum power efficiency ($\eta_{p.\,max}$) of 39.5 lm W^{-1}, and a maximum external quantum efficiency ($\eta_{ext.\,max}$) of 16.4% photons per electron at a brightness of 179 cd m^{-2}; even at a high brightness of 1000 cd m^{-2} or 10000 cd m^{-2}, η_c is still as high as 35.7 cd A^{-1} or 24.2 cd A^{-1} with Commission Internationale de L'Eclairage (CIE) coordinates of (0.50, 0.48). The small values of efficiency roll-off should be attributed to the sufficiently depressed concentration quenching of emissive core and the good charge-transporting ability of the branching units. The device from **Ir-G2** also exhibits high performances with $\eta_{c.\,max}$ of 38.9 cd A^{-1}, $\eta_{p.\,max}$ of 38.3 lm W^{-1}, and $\eta_{ext.\,max}$ of 15.6%. We note that the EL efficiencies enabled by **Ir-G1** and **Ir-G2** are the highest ever reported for solution-processed orange emissive devices and not far from those of the evaporated PhOLEDs ($\eta_{c.\,max}$ of 57.8 cd A^{-1}, $\eta_{p.\,max}$ of 51.9 lm W^{-1}, and $\eta_{ext.\,max}$ of 20.5%) we recently reported.[16]

Nevertheless, the device with **Ir-G3** as emission layer suffered a severe drop in performances with $\eta_{c.\,max}$ of 7.6 cd A^{-1}, $\eta_{p.\,max}$ of 5.4 lm W^{-1}, and $\eta_{ext.\,max}$ of 3.0%. The decreased efficiencies could be rationalized by the following two factors: i) according to the molecule modeling, the directional energy transfer from the outer-dendrons to the emissive center becomes less efficacious as the molecular radius increases from 14 Å for **Ir-G1** to 20 Å for **Ir-G2** and 26 Å for **Ir-G3**; ii) the triplet excitons on triphenylamine units may annihilate as the distance between the two triphenylamine units is within 4−5 Å.[17] The amounts of such contacts (4−5 Å) among the outer dendrons increase sharply from 30 units in **Ir-G2** to nearly 300 units in **Ir-G3** (Figure S3, see the Supporting Information), thus much more annihilation of triplet excitons on triphenylamine units may occur in **Ir-G3**. The increased close contacts also make against the energy transfer from the outer-dendrons to the emissive core. This assumption is consistent with the PL experimental results that **Ir-G3** exhibits nonmonoexponential decay profiles (Figure 5) and relative

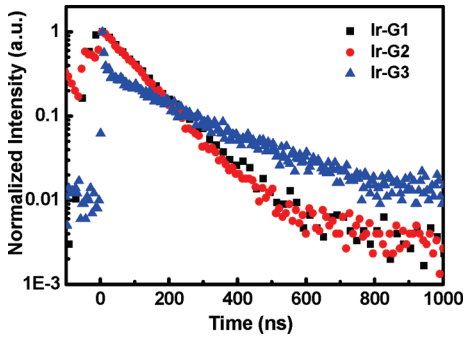

Figure 5. Transient photoluminescence decay of the dendrimers.

long PL lifetime (16.7 and 36.4 ns, Table 1) compared with **Ir-G1** and **Ir-G2** with monoexponential decay profiles and relative short PL lifetimes of ca. 10 ns (Table 1).[6e]

Doped Orange Electrophosphorescence. For comparison, we also prepared a control device under the identical conditions except using **Ir-G1** as guest blended with the general polymer matrix containing poly(*N*-vinylcarbazole) (PVK) and electron-transport material 2-*tert*-butylphenyl-5-biphenyl-1,3,4-oxadiazol (PBD) with the ratio of PVK (72 wt %):PBD (21 wt %):**Ir-G1** (7 wt %) as emissive layer. The device acquires $\eta_{c.\,max}$ of 41.7 cd A^{-1} and $\eta_{ext.\,max}$ of 16.7% at a brightness of 253 cd m^{-2} (Figure 6), which are comparable with those of the self-hosted device from **Ir-G1**. Similarly, when the luminance reaches 1000 cd m^{-2}, the efficiencies are still high: η_c of 38.3 cd A^{-1} and η_{ext} of 15.3%. However, its maximum power efficiency of 13.6 lm W^{-1} is much lower than the latter (39.5 lm W^{-1}) due to its high turn-on voltage of 7.2 V. We believe that the

dx.doi.org/10.1021/cm202732j | *Chem. Mater.* 2012, 24, 174−180

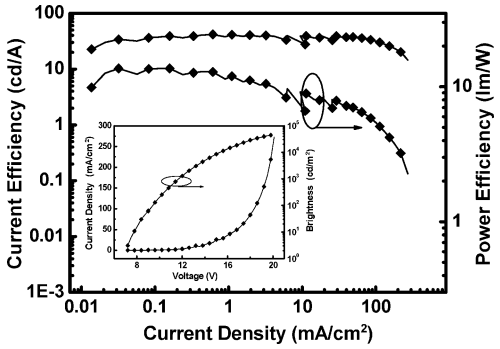

Figure 6. Current/power efficiency versus current density curve and *J*–*V*–*L* characteristic (inset) for doped orange electrophosphorescence using **Ir-G1** as phosphor.

suppressed interaction between emissive cores as well as the good charge-injection and transporting capabilities of peripheral triphenylamine units make the orange EL device with neat iridium dendrimer as emissive layer superior performance that exceeded that of the traditional host–guest system.

CONCLUSIONS

In conclusion, we have developed a convenient and robust convergent synthesis for phosphorescent dendrimers. Facile preparation of large dendritic ligands without structural defect as well as thereafter efficient complexation with iridium source renders the iridium dendritic phosphors feasible in real application of organic electronics. Bearing excellent hole-transporting ability, the functional dendrons not only act as good spacers isolating the Ir complex core but also participate straightforwardly in charge injection, transport, and energy transfer. The device results indicate that the first generation of double-dendron Ir dendritic array is structurally enough for solution-processable host-free phosphors. This demonstrates that the new iridium dendritic architectures with appropriate dendron and generation numbers are excellent self-host–guest system at the molecular level. With the best performances recorded so far for solution-processed orange PhOLEDs, we believe that this powerful synthetic strategy and efficient triphenylamine-dendron system would have great potential to construct novel phosphorescent dendrimers that have emission colors covering the whole visible region for use in full-color displays or white-emitting PhOLEDs.

ASSOCIATED CONTENT

Supporting Information

Figures S1–S3.This material is available free of charge via the Internet at http://pubs.acs.org.

AUTHOR INFORMATION

Corresponding Author

*E-mail: clyang@whu.edu.cn (C.Y.); hbwu@scut.edu.cn (H.W.).

ACKNOWLEDGMENTS

C. Yang thanks the National Science Fund for Distinguished Young Scholars of China (No. 51125013), the National Natural Science Foundation of China (90922020), the National Basic Research Program of China (973 Program 2009CB623602), and the Fundamental Research Funds for the Central Universities of China. H. Wu thanks the National Natural Science Foundation of China (61177022); J. Zou thanks China Postdoctoral Science Foundation (201104352) for financial support.

REFERENCES

(1) D'Andrade, B. W.; Forrest, S. R. *Adv. Mater.* **2004**, *16*, 1585.
(2) Baldo, M. A.; O'Brien, D. F.; You, Y.; Shoustikov, A.; Sibley, S.; Thompson, M. E.; Forrest, S. R. *Nature* **1998**, *395*, 151.
(3) Holder, E.; Langeveld, B. M. W.; Schubert, U. S. *Adv. Mater.* **2005**, *17*, 1109.
(4) (a) Tsuboyama, A.; Iwawaki, H.; Furugori, M.; Mukaide, T.; Kamatani, J.; Igawa, S.; Moriyama, T.; Miura, S.; Takiguchi, T.; Okada, S.; Hoshino, M.; Ueno, K. *J. Am. Chem. Soc.* **2003**, *125*, 12971. (b) Wong, W.-Y.; Ho, C.-L.; Gao, Z.; Mi, B.; Chen, C.-H.; Cheah, K.-W.; Lin, Z. *Angew. Chem., Int. Ed.* **2006**, *45*, 7800. (c) Tao, Y.; Wang, Q.; Yang, C.; Wang, Q.; Zhang, Z.; Zou, T.; Qin, J.; Ma, D. *Angew. Chem., Int. Ed.* **2008**, *47*, 8104. (d) Tao, Y.; Yang, C.; Qin, J. *Chem. Soc. Rev.* **2011**, *40*, 2943. (e) Gong, S.; Fu, Q.; Wang, Q.; Yang, C.; Zhong, C.; Qin, J.; Ma, D. *Adv. Mater.* **2011**, *23*, 4956.
(5) Reineke, S.; Walzer, K.; Leo, K. *Phys. Rev. B* **2007**, *75*, 125328.
(6) (a) Lo, S.-C.; Male, N. A. H.; Markham, J. P. J; Magennis, S. W.; Burn, P. L.; Salata, O. V.; Samuel, I. D. W. *Adv. Mater.* **2002**, *14*, 975. (b) Lo, S.-C.; Namdas, E. B.; Burn, P. L.; Samuel, I. D. W. *Macromolecules* **2003**, *36*, 9721. (c) Ding, J.; Lü, J.; Cheng, Y.; Xie, Z.; Wang, L.; Jing, X.; Wang, F. *Adv. Funct. Mater.* **2008**, *18*, 2754. (d) Qin, T.; Ding, J.; Wang, L.; Baumgarten, M.; Zhou, G.; Müllen, K. *J. Am. Chem. Soc.* **2009**, *131*, 14329. (e) Lo, S.-C.; Harding, R. E.; Shipley, C. P.; Stevenson, S. G.; Burn, P. L.; Samuel, I. D. W. *J. Am. Chem. Soc.* **2009**, *131*, 16681.
(7) (a) Ding, J.; Gao, J.; Cheng, Y.; Xie, Z.; Wang, L.; Ma, D.; Jing, X.; Wang, F. *Adv. Funct. Mater.* **2006**, *16*, 575. (b) Zhou, G.; Wong, W.-Y.; Yao, B.; Xie, Z.; Wang, L. *Angew. Chem., Int. Ed.* **2007**, *46*, 1149. (c) Lo, S.-C.; Bera, R. N.; Harding, R. E.; Burn, P. L.; Samuel, I. D. W. *Adv. Funct. Mater.* **2008**, *18*, 3080. (d) Ding, J.; Wang, B.; Yue, Z.; Yao, B.; Xie, Z.; Cheng, Y.; Wang, L.; Jing, X.; Wang, F. *Angew. Chem., Int. Ed.* **2009**, *48*, 6664.
(8) Lo, S.-C.; Burn, P. L. *Chem. Rev.* **2007**, *107*, 1097.
(9) (a) Wong, W.-Y.; Zhou, G.; Yu, X.; Kwok, H.-S.; Tang, B. *Adv. Funct. Mater.* **2006**, *16*, 838. (b) Wong, W.-Y.; Zhou, G.; Yu, X.; Kwok, H.-S.; Lin, Z. *Adv. Funct. Mater.* **2007**, *17*, 315. (c) Zhou, G.; Ho, C.-L.; Wong, W.-Y.; Wang, Q.; Ma, D.; Wang, L.; Lin, Z.; Marder, T. B.; Beeby, A. *Adv. Funct. Mater.* **2008**, *18*, 499. (d) Wu, H.; Zhou, G.; Zou, J.; Ho, C.-L.; Wong, W.-Y.; Yang, W.; Peng, J.; Cao, Y. *Adv. Mater.* **2009**, *21*, 4181.
(10) Imaoka, T.; Tanaka, R.; Arimoto, S.; Sakai, M.; Fujii, M.; Yamamoto, K. *J. Am. Chem. Soc.* **2005**, *127*, 13896.
(11) Pudzich, R.; Salbeck, J. *Synth. Met.* **2003**, *138*, 21.
(12) (a) Miyaura, N.; Suzuki, A. *Chem. Rev.* **1995**, *95*, 2457. (b) Klapars, A.; Antilla, J. C.; Huang, X.; Buchwald, S. L. *J. Am. Chem. Soc.* **2001**, *123*, 7727.
(13) Tamayo, A. B.; Alleyne, B. D.; Djurovich, P. I.; Lamansky, S.; Tsyba, I.; Ho, N. N.; Bau, R.; Thompson, M. E. *J. Am. Chem. Soc.* **2003**, *125*, 7377.
(14) Zhou, G.; Wong, W.-Y.; Yao, B.; Xie, Z.; Wang, L. *J. Mater. Chem.* **2008**, *18*, 1799.
(15) Sajoto, T.; Djurovich, P. I.; Tamayo, A. B.; Oxgaard, J.; Goddard, W. A.; Thompson, M. E. *J. Am. Chem. Soc.* **2009**, *131*, 9813.
(16) Gong, S.; Chen, Y.; Yang, C.; Zhong, C.; Qin, J.; Ma, D. *Adv. Mater.* **2010**, *22*, 5370.
(17) Zeng, Y.; Li, Y.-Y.; Chen, J.; Yang, G.; Li, Y. *Chem. Asian J.* **2010**, *5*, 992.